

Fredrik During^{1,2}, Raghu Chaitanya Munjulury^{1,3} & Robert Hällqvist^{1,4}

¹Division of Fluid and Mechatronic Systems (FLUMES), Linköping University, Sweden
 ²Structural Design, Saab Aeronautics, Sweden
 ³Design Methodology, Saab Aeronautics, Sweden
 ⁴System Simulation and Concept Development, Saab Aeronautics, Sweden

Abstract

Modelling complex mechanical systems during product development phases challenges the most ingrained engineers and tracking evolving system requirements, design configurations, and version control are key for success. Conflicting requirements force trade-offs between domains, often based on insight gained from system models as its foundation. Hence, the efficient flow of information from system models to all domains is of the highest importance. Methodologies such as Model-Based System Engineering (MBSE) emphasise utilisation of the information contained inside models, to make the models themselves the main information carriers thereby increasing the efficiency with which information can propagate between domains. The automated creation of selected digital artefacts along with standardised formatting can create robust connections between specialised engineering tools needed for MBSE adoption within the design engineering field and industry. The Functional Mock-up Interface (FMI) and System Structure and Parameterization (SSP) standards have been shown to be viable standardized formats for information propagation between Computer Aided Design (CAD) and system simulation tools. However, the application of such standards for geometrical design processes is still in its infancy, and more research is needed to prove its usability and to establish corresponding methodologies in an industry setting. The results presented in this paper show that the automatic generation of input parameters used as the foundation for deterministic simulations can be done for both new and legacy CAD models of a Coolant Distribution System (CDS). The developed automation framework is through integrated engineering knowledge enabled by Knowledge-Based Engineering (KBE) methods, able to estimate the pressure loss coefficient for pipes, hoses, and couplings as well as other needed simulation input parameters from the CAD model of the CDS used as an application example. By mapping the topology of the geometrical CAD model to the simulation components representing the CDS model, the automation framework is able to aggregate and sort simulation input parameters ready to be propagated according to the SSP standard. The work shows that by using automation frameworks, and including necessary engineering knowledge into the geometrical CAD models, MBSE adoption is possible in the field of geometrical design.

Keywords: Automation, KBE, MBSE, CAD, FMI, SSP

1. Introduction

For the development of complex systems, systems defined as a whole consisting of interacting parts, structure, and methodology are keys to success. The ability to keep track of evolving system requirements throughout a system's life cycle is a challenge. Systems Engineering (SE) is an iterative and interdisciplinary approach to developing such complex systems, focusing on the documentation of requirements, and continuing through design synthesis and system validation. MBSE has been stated to be the logical successor of SE where modelling activities have been incorporated to support the requirements, design, analysis, and Verification & Validation (V&V) activities throughout its life cycle. By pivoting from data management in manually updated digital artefacts used in SE, to data

management within the models themselves, MBSE aims to improve consistency and communication between stakeholders [1].

Within engineering, different engineering tools are preferable for different tasks, for example, mechanical design or analysis. Sometimes one Swiss army knife toolbox can be utilized for a multitude of activities, but this might not be possible nor desirable in other cases. In some cases, it is preferred to use the best tool for each engineering task. This was the case for Saab Aeronautics during the development of the Gripen E and F fighter jets. The choice was made to apply different specialised tools in a MBSE methodology [2]. However, the use of different engineering tools provided by different vendors in the same development project presents a challenge within the MBSE approach, as tools evolve at different rates and maintaining useful connections between them requires substantial maintenance. In the Gripen E and F project this problem was solved by a partial implementation of the MBSE methodology where models were extensively used: however, data management and propagation were often based on traditional manually written documentation. Manual exchange of data is tedious, error-prone, and may result in fewer data exchanges between disciplines being made than optimal, which can limit the simulation model's credibility [3]. Regardless, successful implementation was achieved, but the possibile for models to themselves carry their own embedded configuration data and the ability for this data to propagate to other models with different frames of reference was identified as a possible area of improvement [2].

For stable connection between engineering tools and distribution of data between models, standardised formats for the integration of digital artefacts are essential according to the Intentional Organisation for Standardisation (ISO) [4]. The SSP and FMI standards aim to provide such standardised formats for interoperability between tools. In short, the FMI standard focuses on the standardised packaging of simulation models into a Functional Mock-up Unit (FMU) for export [5], whilst the SSP standard focuses on standardised connections between models and structure regarding model parameters [6]. Within mechanical engineering, CAD is always part of the design process for complex mechanical systems. In addition, mathematical models representing the physical function and interaction between components are often used for the V&V of the design. To achieve further MBSE methodology adoption within geometrical modelling, propagation of the configuration and geometrical data contained in the geometrical CAD model, that is geometry that affects the system's behaviour, is needed. Since the models are the main information carriers in the MBSE methodology, the focus of document control is replaced by the need for control over the model evolution [7]. A proposed methodology for simulation parameter generation from geometrical CAD models must be able to return a set of predetermined parameters deterministically and be able to exchange this data between engineering tools through for example SSP standardised packaging. To be relevant in an industry setting with long product life cycles, such a methodology must also be able to operate under strict version control of any utilised digital artefact, as well as requiring minimal alteration to enable functionality with legacy models.

The presented work is a continuation of research published in *Realizing Interoperability between MBSE Domains in Aircraft System Development* [8]. In the article, the authors discuss the possibility of applying the SSP 1.0 standard in its current form in an industry setting to verify its usability. Hällqvist et al. conclude that the SSP standard has great potential to contribute to an efficient and automated method for multi-domain interoperability for mechanical system models during development and throughout their life cycles. The authors demonstrate an implementation where the mechanisms of the SSP standard are exploited to establish automated interoperability between geometry and system simulation models. The technology was demonstrated through two different configurations of a CDS where some simulation parameters were extracted from a geometrical CAD model, using KBE, and propagated to a system simulation model. The two evaluated configurations of the CDS used were (a) and (b), as shown in Figure 1 and described further in Section 3. The presented work is carried out to fill a subset with remaining gaps in the parameter extraction from the two CDS models.

1.1 Contributions

The presented work entails a summation of a master thesis within KBE conducted at Saab Aeronautics & Linköping University [9]. The main result of the thesis is a proposed methodology for the estimation of pressure loss coefficients based on geometrical CAD models of internal flow systems.

The constituent parts of the CDS analysed for the estimation of the pressure loss coefficient are pipes, hoses, and connections. Additional functionalities implemented are the ability to estimate the length of the routing, insulation coverage, and features to aid the user in complying with version control when updating legacy geometrical CAD models for automation.

2. Theoretical Background

This article describes techniques to automatically and deterministically estimate the pressure loss coefficient of internal flow systems with a circular cross-section. Consideration has not been taken to the expansion or stretching of parts due to pressure within the CDS. The estimations are based on the geometry available in the in CAD models of the CDS in CATIA V5. The necessary theory is detailed below and is mainly based on handbook equations made available in *Internal Flow Systems* [10].

2.1 Turbulent Flow

The nature of turbulent flow with its ever-changing eddies makes engineering practices a challenge since no consistent boundary condition can be determined [10]. The unitless Reynolds number

$$Re = \frac{UD}{v} = \frac{4\dot{m}}{\pi\mu d} \tag{1}$$

describes the interactions between the fluids' internal and viscous forces. Due to the fluids' viscosity and the roughness of the flow system internal wall material, the fluid in the direct vicinity of the pipe walls sticks and comes to rest. The layer of stationary fluid created is called the boundary layer.

2.2 Adverse Gradient

The denotation adverse gradient is used to describe the region where static pressure increases in the direction of the flow [10]. In other words, the region where the fluid has significantly lower velocity and dynamic pressure than the mean value of the flow. When an energy-deficient fluid enters a region of high static pressure, a conversion of velocity pressure into static pressure occurs. This requires either a supply of energy from the higher energy parts of the flow further away from the walls, or for the fluid to come to rest by giving up all its velocity energy. Once parts of the flow are brought to a velocity of zero, the flow is said to have stalled or separated and creates areas of reverse flow that continue downstream for some distance. To redevelop the flow, a major mixing of the fluid occurs to reach energy equilibrium within the flow. In this redevelopment phase, a major part of the losses occurs for a component.

2.3 Pressure Loss in Internal Flow Systems

System pressure losses are not trivial in their estimation because of the many variables involved. Experimental approaches have often been adopted and methods such as quoting where the pressure loss of components such as valves, bends, orifices, etc. are set equal to the pressure loss for a length of straight pipe, are common [10]. For some flow systems the previous assumptions can be sufficient, however, these heuristic methods do not include the changing losses in components due to the Reynolds number variations. Hence, the introduction of a pressure loss coefficient (z) for all components in the constituent system is advantageous [10]. The introduction of the pressure drop coefficient enables a component's pressure loss to be estimated through its geometry rather than with testing or rule-of-thumb estimations. The pressure loss coefficient can be used to calculate the head loss

$$\Delta H = z \frac{U^2}{2g} \tag{2}$$

as well as the pressure drop

$$\Delta P = z \frac{\rho U^2}{2g} \tag{3}$$

of the component or the system via the superposition principle.

2.4 Pressure Loss — Turing Flows

Changing direction or turning the flow in an internal flow system can be realised by anything from smooth, gradually turning pipes or hoses, to sharp elbow connectors. Regardless of physical implementation, turning the flow with a bend radius smaller than 10 pipe diameters produces two adverse gradients, which promote mixing followed by redevelopment, and thereby produces losses [10]. For turning flows, two parameters are of importance, the radius ratio (r/d), and the bend deflection angle θ_b . The uncorrected pressure loss coefficient for bends z_b^* can then be derived for fixed Reynolds numbers from charts. As turbulent flow is dependent on the Reynolds number and friction, the same is true for the pressure loss coefficient. To account for this, a correction factor C_{Re} and C_f can be used to modify the coefficient. Where the correction factor for the Reynolds number C_{Re} is derived from charts, the correction factor for friction C_f is calculated as

$$C_f = f_{rough}/f_{smooth} \tag{4}$$

where friction coefficient f_{rough} and f_{smooth} are derived using a Moody chart.

To relate the pressure losses to the length available for redevelopment, the correction factor C_o is used. This correction factor is dependent on the distance available for flow redevelopment divided by the outlet pipe diameter (L_o/d) called the outlet ratio and the uncorrected pressure drop coefficient z_b^* . The resulting total pressure drop coefficient for turning flows z_b is calculated as

$$z_b = z_b^* \times C_{Re} \times C_o \times C_f. \tag{5}$$

2.5 Bend-to-Bend Interaction

If two bends are located in close succession, the pressure, and flow distribution from the outlet of the first bend directly interact with the inlet of the second. This creates a need for a correction factor addressing the bend-to-bend interaction C_{b-b} . Neglecting to compensate for the bend-to-bend interaction often leads to an overestimation of the pressure loss as part of the pressure loss attributed to the redevelopment of flow after the first bend no longer has time to occur. To determine the correction factor, C_{b-b} the combination angle θ_b , radius ratio r/d, and spacer ratio L_s/d are of interest. For bends separated by a spacer with a length of more than 30 pipe diameters, the effects of bend-to-bend can be neglected and C_{b-b} can be set to unity [10]. Correction of the pressure loss coefficient regarding the bend-to-bend interaction is done according to

$$z_{b-b} = (z_{b1} + z_{b2})C_{b-b}. (6)$$

2.6 Expansion and Contraction of Flows

The pressure loss coefficient for suddenly expanding flows z_{se} and suddenly contracting flows z_{sc} are calculated as

$$z_{se} = \left(1 - \frac{A_{inlet}}{A_{outlet}}\right)^2 \tag{7}$$

$$z_{sc} = 0.4 \left(1 - \left(\frac{A_{outlet}}{A_{inlet}} \right)^2 \right) \tag{8}$$

and often realised in an internal flow system as adaptor couplings.

3. Method

Included in this section is an overview of how the work was carried out and how the theory was applied. The section starts with a description of the application example, a tool developed for version control, and an outline of the method used to map CAD models to simulation models. The section continues with the method used for the automated pressure loss coefficient estimation as well as other automated extractions of input parameters such as length, insulation coverage, and inlet coordinates.

3.1 Application Example

The data automatically extracted from the geometrical CAD model is, through SSP packaging, tailored to the simulation model created for the application example created and used in [8]. The application example was developed with a sub-system requirement list from a hypothetical development of a radar system requiring cooling. The geometry of the CDS was modelled in two configurations, (a) and (b), shown in Figure 1. The main components in the CDS are the *Air-to-Liquid Heat Exchanger* (LHEX), accumulator, pump, and routing consisting of pipes, hoses, and connectors.

The main difference between the configurations of the CDS is the distance between the distribution core including the pump, accumulator, and LHEX, and the radar. Both configurations could have pros and cons from a design point of view where the placement of the distribution core of configuration (a) could provide some key advantage whilst being penalised due to greater head losses, or vise versa. To aid system designers in the choice of component arrangement, the performance of both configurations needs to be evaluated. The proposed methodology aims to provide a deterministic way to estimate the differences in pressure loss between configurations (a) and (b), caused by the different routing.

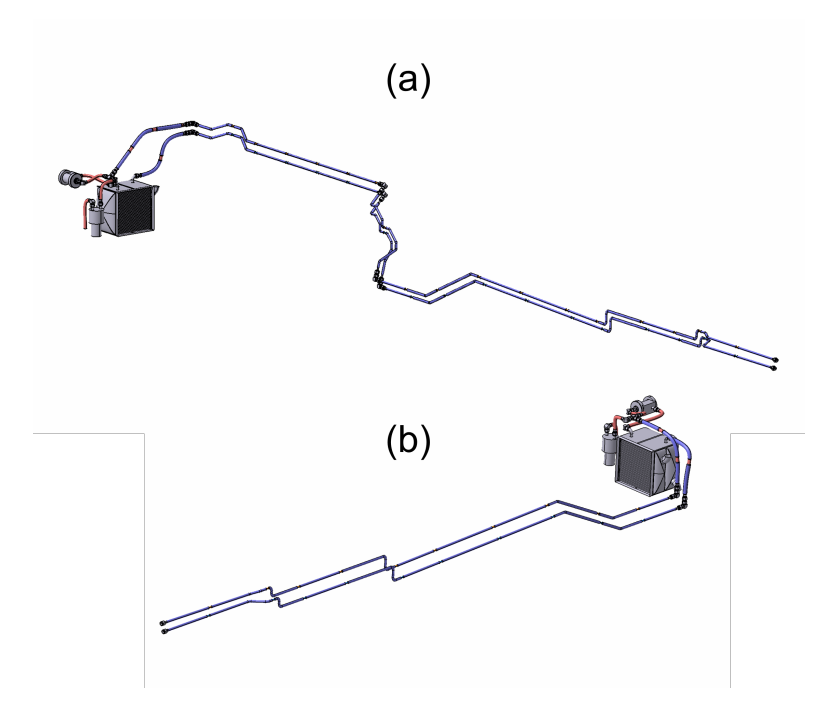


Figure 1 – Two configurations of the Coolant Distribution System CDS, (a) and (b).

3.2 Knowledge Based Engineering

Knowledge-Based Engineering (KBE) is a technology and method of capturing engineering knowledge within engineering models. By exploiting scripts, the captured knowledge can be reused in a fast and integrated way. KBE is mainly used where rule-based models can be created to determine deterministic answers from some manageable amount of input parameters. This enables the automation or semi-automation of repetitive design tasks and can greatly speed up the generation of concepts during development [11][12]. Historically, KBE and CAD have been closely related, and nowadays, most CAD software has this technology embedded. Within CATIA V5, this is called *Knowledgeware* and it can be accessed and used within the program itself or via a separate programming language through an *Application Programming Interface* (API). The method used in the presented work was to use Microsofts programming language *Visual Basic for Applications* (VBA) through the automation API. Some design methodologies have been developed to utilize and manage KBE models, where *Methodology and software tools Oriented to KBE Applications* (MOKA) is one of the more detailed ones. The methodology provides a schema for how to integrate and manage the design knowledge into the models during its entire life cycle [13].

3.3 Version Control and Legacy Models

The work carried out within the avionics industry is highly regulated as a consequence of decades of risk mitigation work. Usually, both domestic and international regulations must be followed for an aircraft to be deemed airworthy. One of many requirements to be deemed airworthy is that all constituent part documentation, including all drawings and specifications, necessary to define the aircraft configuration must be shown to comply with applicable certification [14]. Hence, when working with geometrical CAD models in the avionics industry, version control and traceability are a requirement. The developed automation framework is therefore developed to operate according to these prerequisites.

As legacy models are the backbone of a company's product line-up, proving an automated frameworks usability for these models are identified as the main target of the work. Legacy models are often several years old and have rarely been developed with automation in mind. A method is therefore needed to adapt legacy models to include structured features so that automation through scripts then can be applied. Minimising the amount of changes made to the legacy models is desirable to speed up the revision process. To assist the user in the revision process, functionality for selective editing of specific models included in a larger CAD product was developed. This enables an easier first step in the revision process by duplicating the CAD geometry of interest from the CDS, in this case, the routing, which is the first step in the revision process. The functionality is realised with a script prompting the user to select a product to copy and a destination to paste in the CAD environment. By using a filter, only models in the assembly included in the routing is copied from the original product are pasted whilst preserving the model hierarchies.

3.4 Mapping CAD and Simulation Topology

Simulation models and geometrical CAD models look fundamentally different. In a practical sense, this means that the geometry, in the geometrical CAD model, not necessarily is represented one-to-one in the simulation model. In other words, the topological architecture in the geometrical CAD model and simulation model are often not the same. To enable geometrical CAD and simulation model unification, mapping of CAD geometry to simulation components is necessary. An example of this mapping can be seen in Figure 2 where multiple parts in the geometrical CAD model, who together create the return line in the CDS, are mapped to a single simulation component in the simulation model.

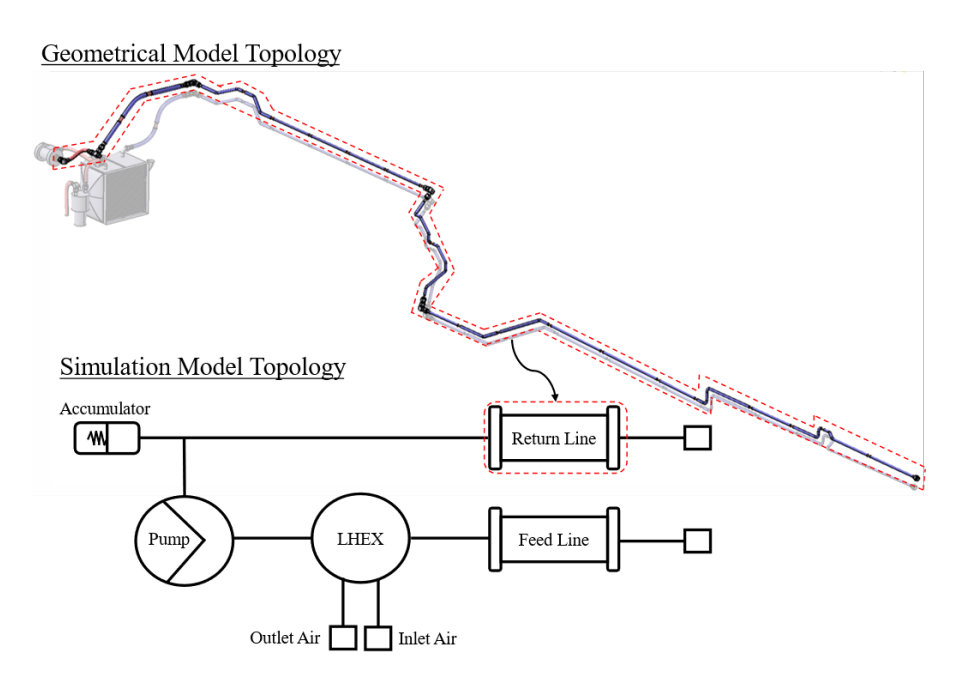


Figure 2 – Example of mapping multiple geometrical CAD parts to a single simulation component in the simulation model.

As model development requires specialised expertise, the geometrical design model and simulation model are often developed and maintained independently of each other. This asynchronous model evolution hence requires a reliable, flexible, and traceable mapping between the simulation and geometrical topologies to enable unification throughout the system life cycle. The method implemented to realise the mapping was with an intermediate summation file. The summation file was created as a worksheet in Microsoft Excel and is henceforth referred to as *SummarySheet*. The *SummarySheet* connected the simulation components with its constituent parts in the CAD model by manually paring geometrical model identifiers to the identifiers of the simulation components. Although tedious, this method offers great flexibility and creates a good overview for the user. The *SummarySheet* acts much like the *System Structure Parameter Mapping* (SSM) file within the SSP standard where the SSM file is a formatted *Extensible Markup Language* (XML) [6]. For greater interoperability the *SummarySheet* could be replaced by a SSM file. However, to reduce the scope of the presented work, this was not implemented.

3.5 Estimation of Correction Factor for Reynolds Number

The Reynolds number is unavailable when estimating the pressure loss coefficients for the geometrical CAD model, since mass flow is a result calculated during the performance simulation. The user is however assumed to be able to provide an operational span of mass flow for the CDS extrapolated from system requirements. To estimate the correction factor, C_{Re} an average C_{Re} is calculated based on the operational span of the mass flow specified by the user. By prompting the user to input a minimum and maximum mass flow (in) and absolute viscosity (μ) , two Reynolds numbers are calculated according to Equation 1 with the diameter (d) in the CAD model for the analysed part. An average of the two Reynolds numbers is used in conjunction with the radius ratio (r/d) extracted from the CAD model to calculate the correction factor C_{Re} for the part.

3.6 Estimation of Correction Factor for Friction

Friction is estimated by the simulation model in this application example, and thereby the correction factor C_f , see Equation 4, is set equal to unity. The length of the pipes or hoses is a requirement for this estimation, and thus a script is implemented to automatically extract these parameters from the geometrical CAD model.

3.7 Pressure Loss Estimation of Pipes and Hoses

The definition of a bending pipe or hose is a section whose radius ratio is smaller or equal to $10 (r/d \le 10)$ [10]. This results in pipe and hose-sections with big turning radii compared to their internal diameter are considered as straight segments. Estimation of the pressure loss coefficient for the pipes and hoses is done part-by-part, meaning the part model is opened in CATIA V5, the script is executed, and the new updated part file is saved. This process is repeated for all hoses and pipes in the CDS. Since the pipes and hoses in the CDS have continuous inner diameters, and friction is handled inside the simulation model, the remaining features contributing to the pressure loss coefficient are the bends. Hence, the automation framework is developed to be able to estimate the pressure loss coefficient caused by bends (z_b) in pipes and hoses. The references used by the automation framework for the estimation are the points and curves used to model the pipe or hose. By placing these references in a predetermined location, in this case, a geometrical set named *Published Set*, they can be accessed by the script. Additional measuring points are then added by a script to mesh the centerline of the pipe or hose geometry. To reduce the number of meshing points needed, a method is developed where the length between the original modelling references governs the meshing fidelity for different segments of the pipe or hose geometry.

All measurement geometry is instantiated through *User Defined Features* (UDF) on top of the existing geometry in the geometrical CAD model. A UDF is a programmable tool in CATIA V5 that can perform automatic tasks such as part and parameter manipulation within the part model by instantiating the UDF [15]. All measurement geometry instantiated from the UDF is placed in a new separate geometrical set called *instantiatedGeometry* and has no impact on the shape of the original geometry. The automated pressure loss estimation is performed by a script in four stages, described below.

- 1. Start the script. Geometrical sets *Published Set* and *instantiatedGeometry* are created. The user is prompted to place the references from the model into the *Published Set* as well as enter input data minimum mass flow, maximum mass flow, and absolute viscosity in created parameters in CATIA V5.
- 2. Meshing points are placed along the centerline of the geometry from a UDF with spacing governed by the distance to the next reference in the *Published Set*. An angle measurement is taken between all meshing points, by a measurement UDF, to evaluate the local deflection angle for each segment. Segments with deflection angles over a threshold value are saved. Subsequent saved segments are aggregated to larger segments and saved as possible bends. A measurement UDF is instantiated to determine if the segment saved as a possible bend fulfils the bend definition of $r/d \leq 10$. If fulfilled, the segment is saved as a bend.
- 3. The radius ratio and the total deflection angle for each saved bend are used to determine the uncorrected pressure loss coefficient for each bend. The input data from the mass flows and absolute viscosity parameters are used to determine the correction factor for the Reynolds number C_{Re} . The distances between the segments identified as bends are measured by instantiating a UDF and in conjunction with the combination angles between subsequent bends the bend-to-bend interaction is derived between each bend. With the same measurement UDF, the distance from the last bend to the outlet is measured, to derive the correction factor for the outlet length C_o . The pressure loss coefficient for the modelled part is calculated as

$$z_b = (z_{b,1}^* + z_{b,2}^* + \dots + z_{b,n}^* \times C_o) \times C_{b-b,avg} \times C_{Re} \times C_f$$
(9)

where $C_{b-b,avg}$ is the average of all correction factors for bend-to-bend interactions in the modelled geometry and C_f is set to unity.

4. The estimated pressure loss coefficient and correction factors are saved in the CAD part file as parameters. The previous steps are performed for all pipes and hoses in the CDS.

When the pressure loss coefficients are estimated for all constituent pipes and hoses in the CDS, aggregation of the pressure loss coefficient for all pipe and hose geometry, included in the different simulation components, is done in the *SummarySheet*. This generates the total pressure loss coefficient contribution from pipes and hoses for each simulation component.

3.8 Pressure Loss Estimation of Couplings

Couplings are commonly used in internal flow systems to connect different segments of pipes and hoses. Although there are many types of couplings, their geometry is largely consistent for the same type of coupling. Information regarding the pressure loss coefficients can be provided by the manufacturer or easily estimated with textbook formulas. To reduce complexity, fixed pressure loss coefficients are set for the most occurring internal diameter for each type of coupling in the CDS. The pressure loss coefficients used for the different types of couplings are displayed in Table 1. Two simplifications are made to reduce complexity further. Firstly, T-shaped and 90° bending couplings were assigned the same pressure loss coefficient, calculated with Equation 9. Secondly, straight, suddenly expanding, and suddenly contracting couplings are assigned the same pressure loss coefficient calculated as an average of Equation 7 and 8.

Table 1 – Values of pressure loss coefficients used for the couplings in the CDS.

Coupling	Pressure Loss Coefficient
$z_{b,90^{\circ}}=z_T$	0.16
$z_s = z_{se} = z_{sc}$	0.15

To estimate the pressure loss coefficients for the constituent couplings in the CDS, a script is implemented to automatically count the couplings and sort them by type. The total amount of couplings

of a certain type included in each simulation component is then multiplied with the value set for that specific type according to Table 1 and saved in the *SummarySheet*.

3.9 Additional Simulation Parameters

Additional input parameters are needed for the simulation model, such as the total aggregated length of the constituent pipes and hoses in the simulation components, total insulation coverage of the aggregated length, and inlet coordinates for every simulation component. The developed script reads through the geometrical CAD model and makes use of the sorting of references described earlier in Section 3.7 to extract all necessary parameters. The parameters are then saved in the *SummarySheet*.

4. Results

This section details the experiments performed to evaluate the automated estimation methods for pressure loss coefficients described in Section 3. The section starts off by presenting the validation of the method for C_{Re} estimation, followed by experiment design for the validation of C_o and C_{b-b} . Finally, the section ends by presenting the results of the automatically extracted simulation parameters from the geometrical CAD model.

4.1 Validation of C_{Re}

Validation of the estimation method for C_{Re} was carried out by applying the method on a descriptive example and comparing the estimated value against empirical values in the literature [10]. An operational span of mass flow \dot{m} was chosen to be between 0.01 kg/s to 0.5 kg/s. The absolute viscosity was set to $\mu = 1 \times 10^{-2}$ Pa \times s which correlates with water at around 20° , and a pipe inner diameter of d = 20 mm. This resulted in an estimated $C_{Re} = 1.91$ (dashed line) and a mean error of around 9.5 percent in this mass flow span compared to empirical values for the same interval (solid line), visualized in Figure 3. Since the developer of a CDS in an industry setting can be expected to estimate the operational mass flow more accurately by extrapolating from system requirements, the error would likely be lower in industry implementation.

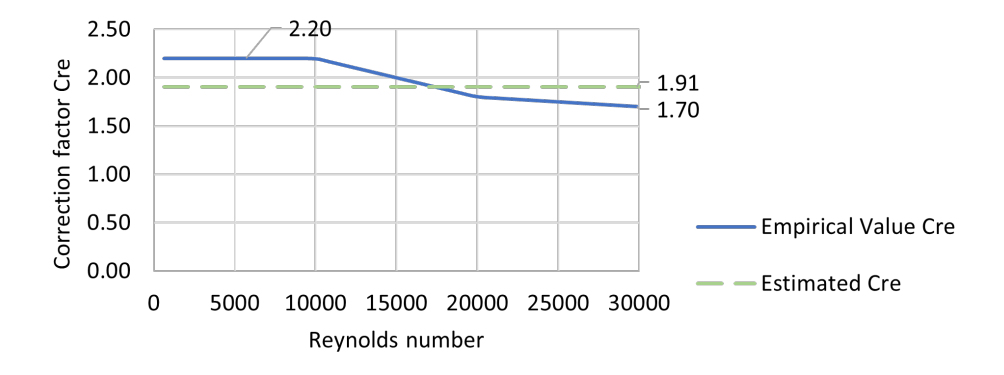


Figure 3 – Estimated correction factor for Reynolds number C_{Re} (dashed line) over a mass flow span of 0.01-0.05 kg/s compared against empirical values (solid line) for the same interval.

4.2 Design of Experiments

To evaluate the accuracy of the automated pressure loss coefficient estimation for pipes and hoses, a series of experiments were designed, which are detailed in the following subsections. The experiments were done by comparing values of pressure loss coefficients and correction factors calculated from empirical values tabulated in the literature [10], to values estimated by the automation framework including correction factors, to values estimated by the automation framework excluding correction factors

For all the experiments, an internal flow system with two bends was modelled in CATIA V5. The deflection angles (θ_b) were set to 90° and the radius ratio (r/d) equal to two for both bends. The mass

flow was set so that the Reynolds number became equal to 10^5 which resulted in a correction factor for Reynolds number C_{Re} to be equal to unity. Extensions were added to the inlet and outlet of the geometrical CAD model so that the flow could be assumed to be fully developed when entering and able to fully redevelop when exiting, resulting in the correction factor for outlet length C_o to be set to unity. Only in the experiment validating the accuracy of the automated estimation of the correction factor C_o did the length of the outlet change in the CAD model.

4.2.1 Validation of C_{b-b}

Different combination angles were tested and the results are visualized in Figure 4. For each combination angle, the pressure loss coefficient is plotted: dark blue as empirical values, light green as automatically estimated values by the framework, and yellow as values automatically estimated by the framework with all correction factors set to unity. The mean error of the framework's automatic estimation of correction factor C_{b-b} compared to empirical values in regard to different combination angles, is around three percent.

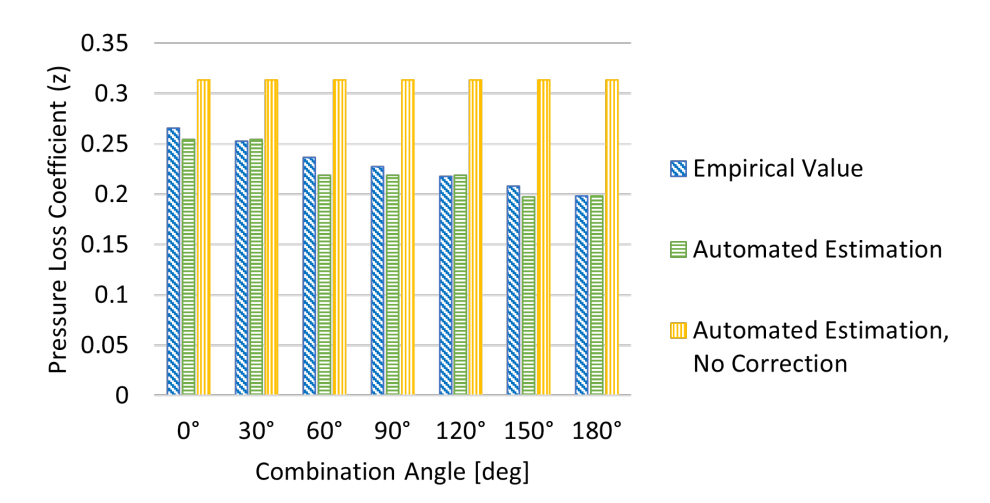


Figure 4 – Pressure loss coefficients dependent on combination angles between 0° to 180°. The calculated pressure loss coefficients are plotted: dark blue as empirical values, light green as automatically estimated values by the framework, and yellow as automatically estimated values by the framework with correction factors set to unity.

4.2.2 Validation Spacer Length

Different spacer lengths were tested and the results are visualized in Figure 5. For each spacer length, the pressure loss coefficient is plotted: dark blue as empirical values, light green as automatically estimated values by the framework, and yellow as values automatically estimated by the framework with all correction factors set to unity. The mean error for the framework's automated estimation of the correction factor C_{b-b} compared to empirical values, in regard to different spacer lengths, is around 10 percent. The reason for the large deviation of the framework estimation at a spacer length of zero pipe diameters is because the developed script erroneously, in this case, identified the two bends in the CAD geometry as one longer continuous bend. This error subsided once the spacer length increased. Excluding the spacer length of zero pipe diameters, the mean error for the framework's automated estimation of the correction factor C_{b-b} compared to empirical values in regard to spacer length, falls to around five percent.

4.3 Output Length

Different output lengths were tested, and the results are visualized in Figure 6. For each outlet length, the pressure loss coefficient is plotted: dark blue as empirical values, light green as automatically estimated values by the framework, and yellow as values automatically estimated by the framework

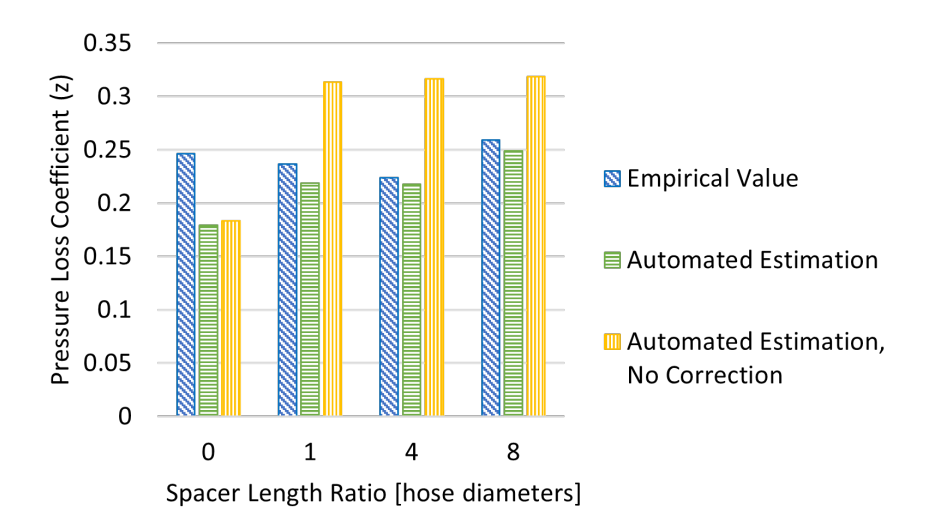


Figure 5 – Pressure loss coefficients dependent on spacer length between zero to eight pipe diameters. The calculated pressure loss coefficients are plotted: dark blue as empirical values, light green as automatically estimated values by the framework, and yellow as automatically estimated values by the framework with correction factors set to unity.

with all correction factors set to unity. The mean error for the framework automatic estimation of the correction factor C_o compared to empirical values in regard to different spacer lengths, is just over five percent.

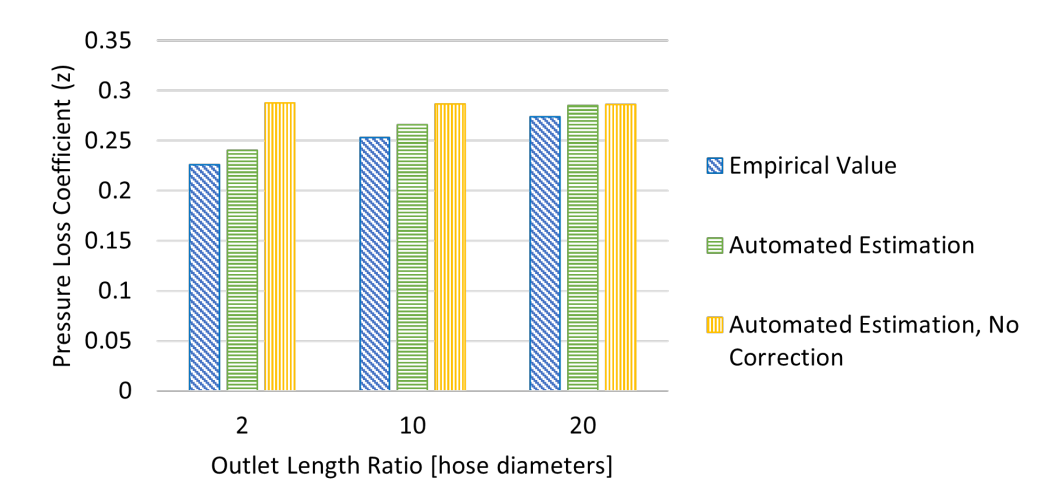


Figure 6 – Pressure loss coefficients dependent on outlet lengths between two and twenty pipe diameters. The calculated pressure loss coefficients are plotted: dark blue as empirical values, light green as automatically estimated values by the framework, and yellow as automatically estimated values by the framework with correction factors set to unity.

4.4 Simulation Parameters

The mapping of geometrical CAD geometry to simulation components in the Microsoft Excel sheet named *SummarySheet* proved to be a sufficient way of merging the two model typologies. The layout of the Excel sheet provided an easy overview of the mapping and substantial flexibility. By utilizing the scripts developed for the automated estimation of pressure loss coefficients and other parameter extraction, each simulation component could be attributed their aggregated simulation input parameters from all its constituent geometrical CAD parts. The topology mapping was limited to the intersection points of the parts in the CAD model.

5. Discussion

The frame of reference used when estimating the pressure loss coefficient for the CDS in this work is part-by-part, meaning the pressure loss coefficient is estimated for each CAD part individually before aggregating them by in the *SummarySheet* by the superposition principle. As a consequence, the flow interactions between each CAD part are not accounted for nor corrected for in the automated estimation. This, in turn, could lead to some inaccuracy in the aggregated pressure loss coefficient estimation of the simulation components, since the effects of the outlet conditions of the last bend in one CAD part is not accounted for in the subsequent CAD part. An overestimation of the simulation components' total pressure loss coefficient would therefore likely occur using the automated framework in its current form, the size of which is dependent on CAD geometry. Future work could be done to adjust the frame of reference so that correction factors for outlet length C_o and bend-to-bend interactions C_{b-b} are done during the aggregation of the pressure loss coefficients for the simulation components. This could improve the accuracy of the estimated values by the framework.

The estimation of the Reynolds number can be expected to generate a source of error when applying the methodology to a real-case scenario. To minimize this error, the estimated operational mass flow span, \dot{m}_{min} and \dot{m}_{max} , for the internal flow system, should be determined as soon as possible in the system development phase. The smaller the estimated mass flow span used as input for the automated framework, the smaller the error for the correction factor for Reynolds number C_{Re} could be expected.

An area neglected in this work is the handling of T-shaped couplings that divide the flow. A method to include the division of flow into the pressure loss coefficient estimation would widen the application scope of the work and enable more complex internal flow systems to be analysed. By establishing the mapping of simulation components to CAD parts to the *SummarySheet* in Microsoft Excel, a flexible and robust workflow was created. The reasoning behind using Microsoft Excel was, apart from the ease of use, the ability to convert data into XML which the SSP standard uses even though formatting would be needed. The mapping utilised in this work in many ways resembles the mapping done by the SSM file used in the SSP standard to map system parameters to simulation components. Future work could be done exploring the possibility of integrating the SSM file directly into the framework to reduce digital artefacts and be more in line with the MBSE approach.

6. Conclusions

Presented in the paper is a method to automatically and deterministically estimate the pressure loss coefficient for an internal flow system. The estimation was made by integrating necessary engineering knowledge through KBE methods to analyse the geometrical CAD model of a CDS, along with extracting simulation input parameters such as length, insulation coverage, and inlet coordinates. By developing an automated framework to analyse pre-existing CAD part geometry, the presented work also shows that both new and legacy CAD models can be altered to benefit from a methodology utilising KBE and automated frameworks.

The work shows that the unification of independently developed CAD and simulation models is possible. The topology of the geometrical CAD model can be mapped to the topology of the simulation model by mapping model identifiers in Microsoft Excel. The proposed method to use a *SummarySheet* where constituent CAD parts in the CDS could be aggregated and mapped in a flexible way to the simulation components proved to be sufficient. The work showed that the tools for interoperability between system simulation and geometrical design already exist. With the implementation of automated frameworks utilising KBE methods, and standardised formats such as SSP and FMI, a more complete implementation of MBSE is possible within the field of geometrical design engineering. Unification of independently developed geometrical CAD models and system simulation models might be around the corner.

7. Contact Author Email Address

Corresponding author: Fredrik During, email: duringfredrik@gmail.com

8. Copyright Statement

The authors confirm that they, and/or their company or organisation, hold copyright on all of the original material included in this paper. The authors also confirm that they have obtained permission, from the copyright holder of any third party material included in this paper, to publish it as part of their paper. The authors confirm that they give permission, or have obtained permission from the copyright holder of this paper, for the publication and distribution of this paper as part of the ICAS proceedings or as individual off-prints from the proceedings.

References

- [1] International Council on Systems Engineering. *Systems Engineering Handbook*. 4th ed. John Wiley and Sons, Inc., 2015.
- [2] Wallén Axehill J and Herzog E. Don't mix the tenses: Managing the present and the future in an mbse context. *Proceedings of the 32nd Annual INCOSE International Symposium*.
- [3] Standards for Models and Simulations, NASA STD-7009, 2008.
- [4] International Organization for Standardization (ISO). ISO 14258:1998/COR 1:2000 Industrial Automation Systems—Concepts and Rules for Enterprise Models—Technical Corrigendum 1, 2023. Accessed: 2023-06-10.
 - URL https://www.iso.org/standard/33536.html
- [5] The Modelica Association Project FMI. Functional mockup interface specification, 2024. Accessed: 2023-06-10.
 - URL https://fmi-standard.org/docs/3.0/
- [6] Modelica Association Project System Structure and Parameterization. System structure and parameterization, 2024. Accessed: 2023-06-10.
 URL https://ssp-standard.org
- [7] Friedenthal S, Moore A and Steiner R. *A Practical Guide to SysML: The Systems Modeling Language*. Burlington, Mass.: Elsevier/Morgan Kaufmann, 2008.
- [8] Hällqvist R, Munjulury R C, Braun R, Eek M and Krus P. Realizing interoperability between mbse domains in aircraft system development. vol. 11, no. 18, 2022.
- [9] During F. Automating Engineering Interoperability: Uniting Geometrical Design and Systems Simulation. Master's thesis, Linköping University, 2023.
- [10] Miller D. Internal Flow Systems. BHRA (Information Services), Cranfield, Bedford, 1990.
- [11] Munjulury R C, Staack I, Berry P and Krus P. A knowledge-based integrated aircraft conceptual design framework. *CEAS Aeronautical Journal*, vol. 7, no. 1, pp. 95–105, 2016.
- [12] Munjulury R C. Knowledge-based integrated aircraft design: An applied approach from design to concept demonstration, 2017.
- [13] Stokes M J. Managing engineering knowledge: Moka-methodology for knowledge based engineering applications. 2001.
- [14] De Florio F. Airworthiness: An Introduction to Aircraft Certification. Elsevier Science, 2006.
- [15] Río-Cidoncha M G D, Martínez-Palacios J and Ortuño-Ortiz F. Task automation for modelling solids with catia v5. *Aircraft Engineering and Aerospace Technology*, vol. 79, pp. 53 59, 2007.